arXiv:1601.01261v1 [math.GM] 3 Jan 2016

A rational approximation of the Dawson's integral for efficient computation of the complex error function

S. M. Abrarov[*] and B. M. Quine[*†]

January 3, 2016

Abstract

In this work we show a rational approximation of the Dawson's integral that can be implemented for high-accuracy computation of the complex error function in a rapid algorithm. Specifically, this approach provides accuracy exceeding $\sim 10^{-14}$ in the domain of practical importance $0 \le y < 0.1 \cap |x + iy| \le 8$. A Matlab code for computation of the complex error function with entire coverage of the complex plane is presented.

Keywords: Complex error function, Faddeeva function, Dawson's integral, rational approximation

1 Introduction

The complex error function also widely known as the Faddeeva function can be defined as [1, 2, 3, 4, 5, 6]

$$w(z) = e^{-z^2}\left(1 + \frac{2i}{\sqrt{\pi}}\int\limits_0^z e^{t^2}dt\right), \tag{1}$$

[*]Dept. Earth and Space Science and Engineering, York University, Toronto, Canada, M3J 1P3.
[†]Dept. Physics and Astronomy, York University, Toronto, Canada, M3J 1P3.

where $z = x + iy$ is the complex argument. It is a solution of the following differential equation [5]

$$w'(z) + 2zw(z) = \frac{2i}{\sqrt{\pi}},$$

where the initial condition is given by $w(0) = 1$.

The complex error function is principal in a family of special functions. The main functions from this family are the Dawson's integral, the complex probability function, the error function, the Fresnel integral and the normal distribution function.

The Dawson's integral is defined as [7, 8, 9, 10, 11]

$$\operatorname{daw}(z) = e^{-z^2} \int_0^z e^{t^2} dt. \tag{2}$$

It is not difficult to obtain a relation between the complex error function and the Dawson's integral. In particular, comparing right sides of equations (1) and (2) immediately yields

$$w(z) = e^{-z^2} + \frac{2i}{\sqrt{\pi}} \operatorname{daw}(z). \tag{3}$$

Another closely related function is the complex probability function. In order to emphasize the continuity of the complex probability function at $\forall y \in \mathbb{R}$, it may be convenient to define it in form of principal value integral [4, 5, 6]

$$W(z) = PV \frac{i}{\pi} \int_{-\infty}^{\infty} \frac{e^{-t^2}}{z - t} dt \tag{4}$$

or

$$W(x, y) = PV \frac{i}{\pi} \int_{-\infty}^{\infty} \frac{e^{-t^2}}{(x + iy) - t} dt.$$

The complex probability function has no discontinuity at $y = 0$ and $x = t$ since according to the principal value we can write

$$\lim W(x, y \to 0) = e^{-x^2} + \frac{2i}{\sqrt{\pi}} \operatorname{daw}(x), \tag{5}$$

where $x = \mathrm{Re}\,[z]$.

There is a direct relationship between the complex error function (1) and the complex probability function (4). In particular, it can be shown that these functions are actually same on the upper half of the complex plain [4, 5]

$$W(z) = w(z), \qquad \mathrm{Im}\,[z] \geq 0. \tag{6}$$

Separating the real and imaginary parts of the complex probability function (4) leads to

$$K(x,y) = PV\frac{y}{\pi}\int\limits_{-\infty}^{\infty}\frac{e^{-t^2}}{y^2+(x-t)^2}dt,$$

and

$$L(x,y) = PV\frac{1}{\pi}\int\limits_{-\infty}^{\infty}\frac{e^{-t^2}(x-t)}{y^2+(x-t)^2}dt, \tag{7}$$

respectively, where the principal value notations emphasize that these functions have no discontinuity at $y = 0$ and $x = t$. In particular, in accordance with equation (3) we can write

$$K(x, y=0) \equiv \lim K(x, y \to 0) = e^{-x^2}$$

and

$$L(x, y=0) \equiv \lim L(x, y \to 0) = \frac{2}{\sqrt{\pi}}\,\mathrm{daw}\,(x)\,.$$

As it follows from the identity (6), for non-negative y we have

$$w(x,y) = K(x,y) + iL(x,y), \qquad y \geq 0. \tag{8}$$

The real part $K(x,y)$ of the complex probability function is commonly known as the Voigt function that is widely used in many disciplines of Applied Mathematics [12, 13, 14], Physics [4, 15, 16, 17, 18, 19, 20, 21] and Astronomy [22]. Mathematically, the Voigt function $K(x,y)$ represents a convolution integral of the Gaussian and Cauchy distributions [5, 15, 16]. The Voigt function is widely used in spectroscopy as it describes quite accurately the line broadening effects [4, 17, 18, 19, 20, 21, 23].

Although the imaginary part $L(x,y)$ of the complex probability function also finds many practical applications (see for example [24, 25]), it has no a specific name. Therefore, further we will regard this function simply as the L-function.

Other associated functions are the error function of complex argument [3, 5]

$$\mathrm{w}(z) = e^{-z^2}\mathrm{erfc}(-iz) = e^{-z^2}[1 - \mathrm{erf}(-iz)] \quad \Leftrightarrow \quad \mathrm{erf}(z) = 1 - e^{-z^2}w(iz),$$

the plasma dispersion function [26]

$$Z(z) = PV\frac{1}{\sqrt{\pi}}\int\limits_{-\infty}^{\infty}\frac{e^{-t^2}}{t-z}dt = i\sqrt{\pi}w(z)$$

the Fresnel integral [3]

$$\begin{aligned} F(z) &= \int\limits_0^z e^{i(\pi/2)t^2}dt \\ &= (1+i)\left[1 - e^{i(\pi/2)z^2}w\left(\sqrt{\pi}(1+i)z/2\right)\right]/2 \end{aligned}$$

and the normal distribution function [27]

$$\begin{aligned} \Phi(z) &= \frac{1}{\sqrt{2\pi}}\int\limits_0^z e^{-t^2/2}dt = \frac{1}{2}\mathrm{erf}\left(\frac{z}{\sqrt{2}}\right) \\ &= \frac{1}{2}\left[1 - e^{-z^2/2}w\left(\frac{iz}{\sqrt{2}}\right)\right]. \end{aligned}$$

Due to a remarkable identity of the complex error function [28, 29]

$$w(-z) = 2e^{-z^2} - w(z),$$

it is sufficient to consider only I and II quadrants in order to cover the entire complex plane (see Appendix A). This property can be explicitly observed by rearranging this identity in form

$$w(\pm x, -|y|) = 2e^{-(\mp x + i|y|)^2} - w(\mp x, +|y|).$$

Thus, due to this remarkable identity of the complex error function we can always avoid computations involving negative argument y by using simply the right side of this equation. Therefore, we will always assume further that $y \geq 0$.

Since the integral on right side of the equation (1) has no analytical solution, the computation of the complex error function must be performed numerically. There are many approximations of the complex error function have been reported in the scientific literature [6, 29, 30, 31, 32, 33, 34]. However, approximations based on rational functions may be more advantageous to gain computational efficiency due to no requirement for nested loop involving decelerating exponential or trigonometric functions dependent upon input the parameters x and y. Although the rational approximations of the complex error function are rapid and provide high-accuracy over the most area of the complex plain, all of them have the same drawback; their accuracy deteriorates with decreasing parameter y (in fact, the computation of the complex error function at small $y << 1$ is commonly considered problematic for high-accuracy computation of the Voigt/complex error function not only in the rational approximations [15, 35, 36]). In this work we propose a new rational approximation of the Dawson's integral and show how its algorithmic implementation effectively resolves such a problem in computation of the complex error function at small $y << 1$.

2 Derivation

In our recent publication [37] we have shown that a new methodology of the Fourier transform results in a rational approximation

$$w\left(z\right) \approx i\frac{2he^{\sigma^2}}{z+i\sigma} + \sum_{n=1}^{N} \frac{A_n - i\left(z+i\sigma\right)B_n}{C_n^2 - \left(z+i\sigma\right)^2}, \tag{9}$$

where the corresponding expansion coefficients are given by

$$A_n = 8\pi h^2 n e^{\sigma^2 - (2\pi h n)^2} \sin\left(4\pi h n \sigma\right),$$

$$B_n = 4he^{\sigma^2 - (2\pi h n)^2} \cos\left(4\pi h n \sigma\right),$$

$$C_n = 2\pi h n$$

and h is the step. In algorithmic implementation it is convenient to rewrite the equation above in form

$$\begin{aligned} \psi(z) &= i\frac{2he^{\sigma^2}}{z} + \sum_{n=1}^{N} \frac{A_n - izB_n}{C_n^2 - z^2} \\ &\Rightarrow w(z) \approx \psi(z + i\sigma). \end{aligned} \tag{10}$$

Using the residue calculus, from approximation (9) we can obtain the rational approximation for the L-function (see Appendix B)

$$L(x) \approx x\left[\frac{2e^{\sigma^2}h}{x^2+\sigma^2} + \sum_{n=1}^{N} \frac{2A_n\sigma + B_n\left(x^2+\sigma^2-C_n^2\right)}{C_n^4 + 2C_n^2\left(\sigma^2 - x^2\right) + \left(x^2+\sigma^2\right)^2}\right]. \tag{11}$$

As $L(x, y = 0) = \mathrm{Im}\left[w(x, y = 0)\right]$ from the identity (3) it follows that

$$\mathrm{daw}(x) = \frac{\sqrt{\pi}}{2}\mathrm{Im}\left[w(x)\right] = \frac{\sqrt{\pi}}{2}L(x).$$

Consequently, according to this identity and equation (11) we can write

$$\mathrm{daw}(x) \approx \frac{\sqrt{\pi}x}{2}\left[\frac{2e^{\sigma^2}h}{x^2+\sigma^2} + \sum_{n=1}^{N} \frac{2A_n\sigma + B_n\left(x^2+\sigma^2-C_n^2\right)}{C_n^4 + 2C_n^2\left(\sigma^2 - x^2\right) + \left(x^2+\sigma^2\right)^2}\right]. \tag{12}$$

Since the argument x is real, it would be reasonable to assume that this equation remains valid for a complex argument $z = x + iy$ as well if the condition $y << 1$ is satisfied. Therefore, substituting the rational approximation of the Dawson's integral (12) into identity (3) results in

$$\begin{aligned} w(z) \approx e^{-z^2} + iz\Bigg[&\frac{2e^{\sigma^2}h}{z^2+\sigma^2} \\ &+ \sum_{n=1}^{N} \frac{2A_n\sigma + B_n\left(z^2+\sigma^2-C_n^2\right)}{C_n^4 + 2C_n^2\left(\sigma^2 - z^2\right) + \left(z^2+\sigma^2\right)^2}\Bigg], \qquad \mathrm{Im}\left[z\right] << 1. \end{aligned} \tag{13}$$

The representation of the approximation (13) can be significantly simplified as given by

$$\begin{aligned} w(z) &\approx e^{-z^2} + 2ihe^{\sigma^2}z\theta\left(z^2+\sigma^2\right) \\ &\Rightarrow \theta(z) \triangleq \frac{1}{z} + \sum_{n=1}^{N} \frac{\alpha_n + \beta_n\left(z - \gamma_n\right)}{4\sigma^2\gamma_n + \left(\gamma_n - z\right)^2}, \quad \mathrm{Im}\left[z\right] << 1, \end{aligned} \tag{14}$$

where the expansion coefficients are

$$\alpha_n = \frac{\sigma}{he^{\sigma^2}} A_n = 8\pi hn\sigma e^{-(2\pi hn)^2} \sin\left(4\pi hn\sigma\right),$$

$$\beta_n = \frac{1}{2he^{\sigma^2}} B_n = 2e^{-(2\pi hn)^2} \cos\left(4\pi hn\sigma\right)$$

and

$$\gamma_n = C_n^2 = (2\pi hn)^2.$$

As we can see from equation (14) only the θ-function needs a nested loop in multiple summation. Therefore, most time required for computation of the complex error function is taken for determination of the θ-function. However, this approximation is rapid due to its simple rational function representation. Although the first term e^{-z^2} in approximation (14) is an exponential function dependent upon the input parameter z, it does not decelerate the computation since this term is not nested and calculated only once. Consequently, the approximation (14) is almost as fast as the rational approximation (10).

3 Implementation and error analysis

The relatively large area at the origin of complex plane is the most difficult for computation with high-accuracy. According to Karbach *et al.* [38] the newest version of the *RooFit* package, written in C/C++ code, utilizes the equation (14) from the work [34] in order to cover accurately this area, shaped as a square with side lengths equal to $2 \times 8 = 16$.

In the algorithm we have developed, instead of the square we apply a circle with radius 8 centered at the origin. This circle separates the complex plane into the inner and outer parts. Only three approximations can be applied to cover the entire complex plain with high-accuracy. The outer part of the circle is an external domain while the inner part of the circle is an internal domain consisting of the primary and secondary subdomains. These domains are schematically shown in Fig. 1.

External domain is determined by boundary $|x + iy| > 8$ and represents the outer area of the circle as shown in Fig. 1. In order to cover this domain we apply the truncated Laplace continued fraction [2, 39, 40, 41]

$$w\left(z\right) = \frac{\mu_0}{z-}\frac{1/2}{z-}\frac{1}{z-}\frac{3/2}{z-}\frac{2}{z-}\frac{5/2}{z-}\frac{3}{z-}\frac{7/2}{z-}..., \qquad \mu_0 = i/\sqrt{\pi}.$$

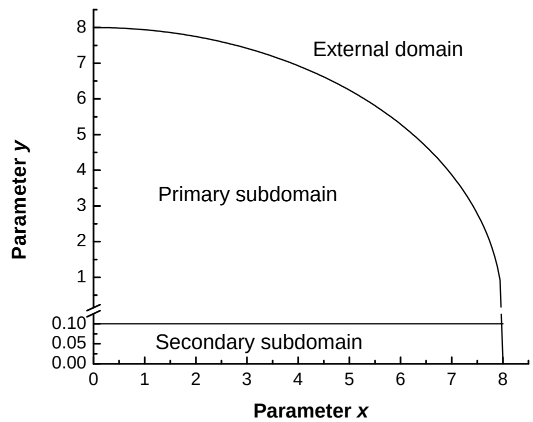

Fig. 1. Domains separating the complex plain for high-accuracy computation of the complex error function.

that provides a rapid computation with high-accuracy. It should be noted, however, that the accuracy of the Laplace continued fraction deteriorates as $|z|$ decreases.

The inner part of the circle bounded by $|x + iy| \leq 8$ is divided into two subdomains. Most area inside the circle is occupied by primary subdomain bounded by $y \geq 0.1 \cap |x + iy| \leq 8$. For this domain we apply the rational approximation (10) that approaches the limit of double precision when we take $N = 23$, $\sigma = 1.5$ and $h = 6/\left(2\pi N\right)$ (see our recent publication [37] for description in determination of the parameter h).

The secondary subdomain within the circle is bounded by narrow band $0 \leq y < 0.1 \cap |x + iy| \leq 8$ (see Fig. 1 along x-axis). The rational approximation (10) sustains high-accuracy within all domain $0 \leq x \leq 40,000 \cap 10^{-4} \leq y \leq 10^2$ required for applications using the HITRAN molecular spectroscopic database [42]. However, at $y < 10^{-6}$ its accuracy deteriorates by roughly one order of the magnitude as y decreases by factor of 10. The proposed approximation (14) perfectly covers the range $y << 1$. In particular, at $N = 23$, $\sigma = 1.5$ and $h = 6/\left(2\pi N\right)$ this approximation also approaches the limit of double precision as the parameter y tends to zero.

In order to quantify the accuracy of the algorithm we can use the relative

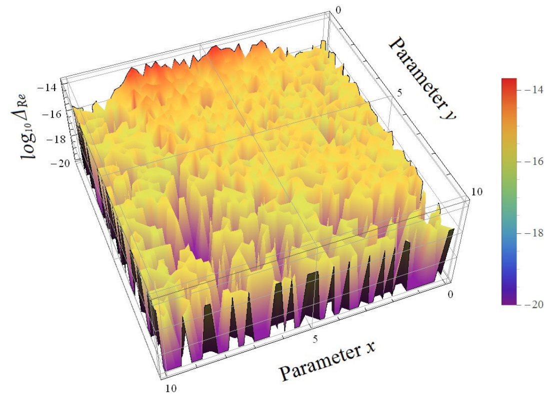

Fig. 2. The logarithm of the relative error $\log_{10}\Delta_{\rm Re}$ for the real part of the algorithm over the domain $0 \le x \le 10 \cap 0 \le y \le 10$.

errors defined for the real and imaginary parts as follows

$$\Delta_{\rm Re} = \left| \frac{{\rm Re}\left[w_{ref}\left(x, y\right)\right] - {\rm Re}\left[w\left(x, y\right)\right]}{{\rm Re}\left[w_{ref}\left(x, y\right)\right]} \right|$$

and

$$\Delta_{\rm Im} = \left| \frac{{\rm Im}\left[w_{ref}\left(x, y\right)\right] - {\rm Im}\left[w\left(x, y\right)\right]}{{\rm Im}\left[w_{ref}\left(x, y\right)\right]} \right|,$$

where $w_{ref}\left(x, y\right)$ is the reference. The highly accurate reference values can be generated by using, for example, Algorithm 680 [40, 41], Algorithm 916 [29] or a recent C++ code in *RooFit* package from the CERNs library [38].

Consider Figs. 2 and 3 illustrating logarithms of relative errors of the considered algorithm for the real and imaginary parts over the domain $0 \le x \le 10 \cap 0 \le y \le 10$, respectively. The rough surface of these plots indicates that the computation reaches the limit of double precision $\sim 10^{-16}$. In particular, while $y > 0.1$ the accuracy can exceed 10^{-15}. However, there is a narrow domain along the along x axis in Fig. 2 (red color area) where the accuracy deteriorates by about an order of the magnitude. Apart from this, we can also see in Fig. 3 a sharp peak located at the origin where accuracy is $\sim 10^{-14}$. Figures 4 and 5 depict these areas of the plots magnified for the real and imaginary parts, respectively.

It should be noted, however, that the worst accuracy $\sim 10^{-14}$ is relatively close to the limitation at double precision computation. Furthermore, since the corresponding areas are negligibly small as compared to the entire inner

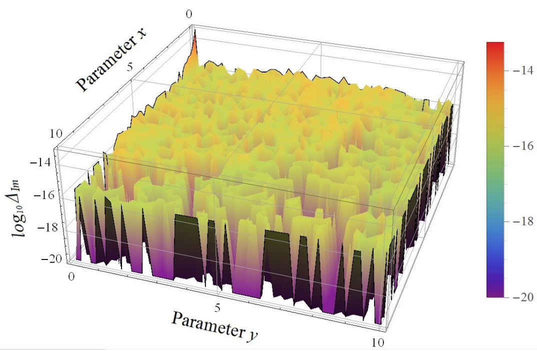

Fig. 3. The logarithm of the relative error $\log_{10}\Delta_{\rm Im}$ for the imaginary part of the algorithm over the domain $0 \le x \le 10 \cap 0 \le y \le 10$.

circle area, where the approximations (10) and (14) are applied, their contribution is ignorable and, therefore, does not affect the average accuracy $\sim 10^{-15}$. Thus, the computational test reveals that the obtained accuracy at double precision computation for the complex error function is absolutely consistent with *CERNLIB*, *libcerf* and *RooFit* packages (see the work [38] for specific details regarding accuracy of these packages).

A Matlab code for computation of the complex error function is presented in Appendix C.

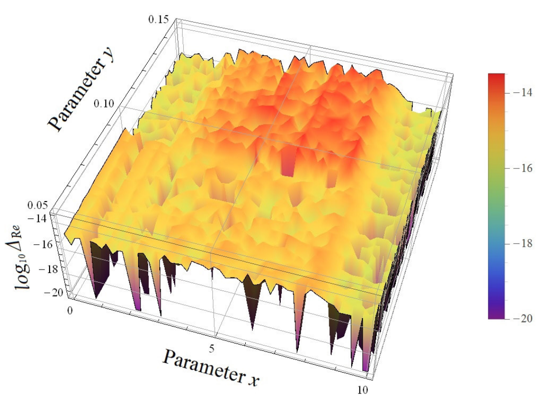

Fig. 4. The logarithm of the relative error $\log_{10}\Delta_{\rm Re}$ for the real part of the algorithm showing the area with worst accuracy $\sim 10^{-14}$.

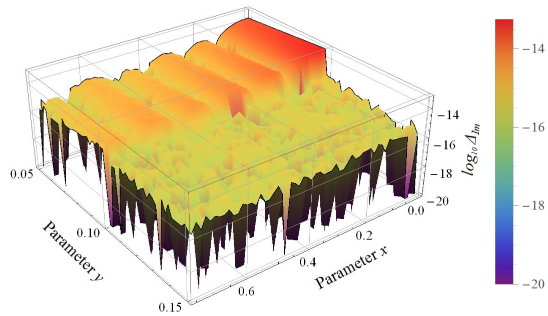

Fig. 5. The logarithm of the relative error $\log_{10}\Delta_{\rm Im}$ for the imaginary part of the algorithm showing the area with worst accuracy $\sim 10^{-14}$.

4 Conclusion

A rational approximation of the Dawson's integral is derived and implemented for rapid and highly accurate computation of the complex error function. The computational test we performed shows the accuracy exceeding $\sim 10^{-14}$ in the domain of practical importance $0 \le y < 0.1 \cap |x+iy| \le 8$. A Matlab code for computation of the complex error function covering the entire complex plane is presented.

Acknowledgments

This work is supported by National Research Council Canada, Thoth Technology Inc. and York University.

Appendix A

It is not difficult to show that the complex error function (1) can be expressed alternatively as (see equation (3) in [12] and [13], see also Appendix A in [11] for derivation)

$$w\left(x,y\right) = \frac{1}{\sqrt{\pi}} \int\limits_{-\infty}^{\infty} \exp\left(-t^2/4\right) \exp\left(-yt\right) \exp\left(ixt\right) dt.$$

Consequently, from this equation we have

$$w(x,y) + w(-x,-y) = \frac{1}{\sqrt{\pi}} \int\limits_{-\infty}^{\infty} e^{-t^2/4} \left[e^{(-y+ix)t} + e^{(y-ix)t} \right] dt$$
$$= \frac{1}{\sqrt{\pi}} \int\limits_{-\infty}^{\infty} e^{-t^2/4} \left[e^{i(x+iy)t} + e^{-i(x+iy)t} \right] dt. \tag{A.1}$$

Using the Euler's identity

$$\frac{e^{i\mu} + e^{-i\mu}}{2} = \cos \mu,$$

where $\mu \in \mathbb{C}$, from the equation (A.1) it follows that

$$w(x,y) + w(-x,-y) = \frac{2}{\sqrt{\pi}} \int\limits_{-\infty}^{\infty} e^{-t^2/4} \cos\left([x+iy]\, t\right) dt = 2e^{-(x+iy)^2}$$

or

$$w(z) + w(-z) = 2e^{-z^2}.$$

Appendix B

As we have shown recently in our publication [43], the real part of the complex error function can be found as

$$\mathrm{Re}\left[w(x,y)\right] = \frac{w(x,y) + w(-x,y)}{2} \tag{B.1}$$

and since [15]

$$\mathrm{Re}\left[w(x,y=0)\right] = K(x,y=0) = e^{-x^2},$$

the substitution of the approximation (9) at $y = 0$ into equation (B.1) leads to

$$e^{-x^2} \approx \frac{2e^{\sigma^2} h\sigma}{x^2 + \sigma^2}$$
$$+ \frac{1}{2} \sum_{n=1}^{N} \left(\frac{A_n - i(x+i\sigma) B_n}{C_n^2 - (x+i\sigma)^2} + \frac{A_n - i(-x+i\sigma) B_n}{C_n^2 - (-x+i\sigma)^2} \right). \tag{B.2}$$

According to the definition of the L-function (7), at $y = 0$ we can write

$$L(x, y = 0) = \lim_{y \to 0} \frac{1}{\pi} \int_{-\infty}^{\infty} \frac{e^{-t^2}(x - t)}{y^2 + (x - t)^2} dt. \tag{B.3}$$

Consequently, substituting the approximation for the exponential function (B.2) into equation (B.3) yields

$$\begin{aligned} L(x, y = 0) \approx \lim_{y \to 0} \frac{1}{\pi} \int_{-\infty}^{\infty} \frac{x - t}{y^2 + (x - t)^2} \Bigg[& \frac{2e^{\sigma^2} h\sigma}{t^2 + \sigma^2} \\ & + \frac{1}{2} \sum_{n=1}^{N} \left(\frac{A_n - i(t + i\sigma) B_n}{C_n^2 - (t + i\sigma)^2} + \frac{A_n - i(-t + i\sigma) B_n}{C_n^2 - (-t + i\sigma)^2} \right) \Bigg] dt. \end{aligned} \tag{B.4}$$

The integrand of the integral (B.4) is analytic everywhere except $2 + 2N$ isolated points on the upper half plane

$$t_r = \{x + iy, i\sigma, -C_n + i\sigma, C_n + i\sigma\}, \qquad n \in \{1, 2, 3, \ \ldots \ N\}.$$

Therefore, using the Residue Theorem's formula

$$\frac{1}{2\pi i} \oint_{C_{ccw}} f(t)\, dt = \sum_{r=1}^{2+2N} \mathrm{Res}\,[f, t_r],$$

where C_{ccw} denotes a contour in counterclockwise direction enclosing the upper half plain (for example as a semicircle with infinite radius) and

$$f(t) = \tfrac{1}{\pi} \times \text{integrand of the integral (B.4)},$$

we obtain the rational approximation (11) of the L-function.

Appendix C

```
function FF = fadfunc(z)

% This program file computes the complex error function, also known as the
% Faddeeva function. It provides high-accuracy and covers the entire
% complex plane. The inner part of the circle |x + i*y| <= 8 is covered by
% the equations (10) and (14). Derivation of the rational approximation
```

```
% (10) and its detailed description can be found in the paper [1]. The new
% approximation (14) shown in this paper computes the complex error
% function at small Im[z] << 1. The outer part of the circle |x + i*y| > 8
% is covered by the Laplace continued fraction [2]. The accuracy of this
% function file can be verified by using C/C++ code provided in work [3].
%
% REFERENCES
% [1] S. M. Abrarov and B. M. Quine, A new application methodology of the
%     Fourier transform for rational approximation of the complex error
%     function, arXiv:1511.00774.
%     http://arxiv.org/abs/1511.00774
%
% [2] W. Gautschi, Efficient computation of the complex error function,
%     SIAM J. Numer. Anal., 7 (1970) 187-198.
%     http://www.jstor.org/stable/2949591
%
% [3] T. M. Karbach, G. Raven and M. Schiller, Decay time integrals in
%     neutral meson mixing and their efficient evaluation,
%     arXiv:1407.0748v1 (2014).
%     http://arxiv.org/abs/1407.0748
%
% The code is written by Sanjar M. Abrarov and Brendan M. Quine, York
% University, Canada, December 2015.

% ************************************************************************
% All parameters in this table are global and can be used anywhere inside
% the program body.
% ------------------------------------------------------------------------
n = 1:23; % define a row vector
sigma = 1.5; % the shift constant
h = 6/(2*pi)/23; % this is the step
% ------------------------------------------------------------------------
% Expansion coefficients for eq. (10)
% ------------------------------------------------------------------------
An = 8*pi*h^2*n.*exp(sigma^2 - (2*pi*h*n).^2).*sin(4*pi*h*n*sigma);
Bn = 4*h*exp(sigma^2 - (2*pi*h*n).^2).*cos(4*pi*h*n*sigma);
Cn = 2*pi*h*n;
% ------------------------------------------------------------------------
% Expansion coefficients for eq. (14)
% ------------------------------------------------------------------------
alpha = 8*pi*h*n*sigma.*exp(-(2*pi*h*n).^2).*sin(4*pi*h*n*sigma);
beta = 2*exp(-(2*pi*h*n).^2).*cos(4*pi*h*n*sigma);
gamma = (2*pi*h*n).^2;
% End of the table
% ************************************************************************
```

```
neg = imag(z)<0; % if imag(z) values are negative, then ...
z(neg) = conj(z(neg)); % ... take the complex conjugate
int  = abs(z)<=8; % internal indices

FF = zeros(size(z)); % define array
FF(~int) = extD(z(~int)); % external domain
FF(int) = intD(z(int)); % internal domain

    function ext_d = extD(z) % the Laplace continued fraction

        coeff = 1:11; % define a row vector
        coeff = coeff/2;

        ext_d = coeff(end)./z; % start computing using the last coeff
        for m = 1:length(coeff) - 1
            ext_d = coeff(end-m)./(z - ext_d);
        end
        ext_d = 1i/sqrt(pi)./(z - ext_d);
    end

    function int_d = intD(z) % internal domain

        secD = imag(z)<0.1; % secondary subdomain indices

        int_d(secD) = exp(-z(secD).^2) + 2i*h*exp(sigma^2)*z(secD).* ...
            theta(z(secD).^2 + sigma^2); % compute using eq. (14)
        int_d(~secD) = rAppr(z(~secD)+1i*sigma); % compute using eq. (10)

        function r_appr = rAppr(z) % the rational approximation (10)

            zz = z.^2; % define repeating array

            r_appr = 2i*h*exp(sigma^2)./z;
            for m = 1:23
                r_appr = r_appr + (An(m) - 1i*z*Bn(m))./ ...
                    (Cn(m)^2 - zz);
            end
        end

        function ThF = theta(z) % theta function (see the eq. (14))

            ThF = 1./z;
            for k = 1:23
                ThF = ThF + (alpha(k) + beta(k)*(z - gamma(k)))./ ...
```

```
                    (4*sigma^2*gamma(k) + (gamma(k) - z).^2);
                end
            end
        end

% For negative imag(z) use the identity w(-z) = 2*exp(-z^2) - w(z)
FF(neg) = conj(2*exp(-z(neg).^2) - FF(neg));
end
```

References

[1] V.N. Faddeyeva, and N.M. Terent'ev, Tables of the probability integral $w(z) = e^{-z^2}\left(1 + \frac{2i}{\sqrt{\pi}}\int_0^z e^{t^2}dt\right)$ for complex argument. Pergamon Press, Oxford, 1961.

[2] W. Gautschi, Efficient computation of the complex error function. SIAM J. Numer. Anal., 7 (1970) 187-198. http://dx.doi.org/10.1137/0707012

[3] M. Abramowitz and I.A. Stegun. Error function and Fresnel integrals. Handbook of mathematical functions with formulas, graphs, and mathematical tables. 9^{th} ed. New York 1972, 297-309.

[4] B.H. Armstrong and B.W. Nicholls, Emission, absorption and transfer of radiation in heated atmospheres. Pergamon Press, New York, 1972.

[5] F. Schreier, The Voigt and complex error function: A comparison of computational methods. J. Quant. Spectrosc. Radiat. Transfer, 48 (1992) 743-762. http://dx.doi.org/10.1016/0022-4073(92)90139-U

[6] J.A.C. Weideman, Computation of the complex error function. SIAM J. Numer. Anal., 31 (1994) 1497-1518. http://dx.doi.org/10.1137/0731077

[7] W.J. Cody, K.A. Paciorek and H.C. Thacher, Chebyshev approximations for Dawson's integral. Math. Comp. 24 (1970) 171-178. http://dx.doi.org/10.1090/S0025-5718-1970-0258236-8

[8] J.H. McCabe, A continued fraction expansion with a truncation error estimate for Dawson's integral, Math. Comp. 28 (1974) 811-816. http://dx.doi.org/10.1090/S0025-5718-1974-0371020-3

[9] G.B. Rybicki, Dawson's integral and the sampling theorem, Comp. Phys., 3 (1989) 85-87. http://dx.doi.org/10.1063/1.4822832

[10] J.P. Boyd, Evaluating of Dawson's integral by solving its differential equation using orthogonal rational Chebyshev functions, Appl. Math. Comput., 204 (2) (2008) 914-919. http://dx.doi.org/10.1016/j.amc.2008.07.039

[11] S.M. Abrarov and B.M. Quine, A rational approximation for the Dawson's integral of real argument, arXiv:1505.04683. http://arxiv.org/pdf/1505.04683.pdf

[12] H.M. Srivastava and E.A. Miller, A unified presentations of the Voigt functions, Astrophys. Space Sci., 135 (1987) 111-118. http://dx.doi.org/10.1007/BF00644466

[13] H.M. Srivastava and M.P. Chen, Some unified presentations of the Voigt functions. Astrophys. Space Sci., 192 (1) (1992) 63-74. http://dx.doi.org/10.1007/BF00653260

[14] G. Pagnini and F. Mainardi, Evolution equations for the probabilistic generalization of the Voigt profile function, J. Comput. Appl. Math., 233 (2010) 1590-1595. http://dx.doi.org/10.1016/j.cam.2008.04.040

[15] B.H. Armstrong, Spectrum line profiles: The Voigt function, 7 (1) (1967) 61-88 J. Quantit. Spectrosc. Radiat. Transfer, http://dx.doi.org/10.1016/0022-4073(67)90057-X

[16] K.L. Letchworth and D.C. Benner, Rapid and accurate calculation of the Voigt function, J. Quant. Spectrosc. Radiat. Transfer, 107 (2007) 173-192. http://dx.doi.org/10.1016/j.jqsrt.2007.01.052

[17] D.P. Edwards, GENLN2: A general line-by-line atmospheric transmittance and radiance model, NCAR technical note, 1992. http://dx.doi.org/10.5065/D6W37T86

[18] B.M. Quine and J.R. Drummond, GENSPECT: a line-by-line code with selectable interpolation error tolerance J. Quant. Spectrosc. Radiat. Transfer 74 (2002) 147-165. http://dx.doi.org/10.1016/S0022-4073(01)00193-5

[19] L.E. Christensen, G.D. Spiers, R.T. Menzies and J.C Jacob, Tunable laser spectroscopy of CO_2 near $2.05\,\mu m$: Atmospheric retrieval biases due to neglecting line-mixing, J. Quant. Spectrosc. Radiat. Transfer, 113 (2012) 739-748. http://dx.doi.org/10.1016/j.jqsrt.2012.02.031

[20] A. Berk, Voigt equivalent widths and spectral-bin single-line transmittances: Exact expansions and the MODTRAN®5 implementation, J. Quant. Spectrosc. Radiat. Transfer, 118 (2013) 102-120. http://dx.doi.org/10.1016/j.jqsrt.2012.11.026

[21] B.M. Quine and S.M. Abrarov, Application of the spectrally integrated Voigt function to line-by-line radiative transfer modelling. J. Quant. Spectrosc. Radiat. Transfer, 127 (2013) 37-48. http://dx.doi.org/10.1016/j.jqsrt.2013.04.020

[22] D. Emerson, Interpreting astronomical spectra. John Wiley & Sons Ltd., 1996.

[23] E. Prince, International tables for crystallography, 3^{rd} ed., Kluwer Academic Publishers, 2004.

[24] N.L. Balazs and I. Tobias, Semiclassical dispersion theory of lasers, Phil. Trans. Royal Soc. A., 264 (1147) (1969) 129. http://dx.doi.org/10.1098/rsta.1969.0002

[25] L.K.P. Chan, Equation of atomic resonance for solid-state optics. Appl. Opt., 25(11), (1986) 1728-730. http://dx.doi.org/10.1364/AO.25.001728

[26] B.D. Fried and S.D. Conte. The plasma dispersion function. New York, Academic Press, 1961.

[27] E.W. Weisstein, CRC concise encyclopedia of mathematics. Chapman & Hall/CRC, 2^{nd} ed. 2003.

[28] S.J. McKenna, A method of computing the complex probability function and other related functions over the whole complex plane. Astrophys. Space Sci., 107 (1) (1984) 71-83. http://dx.doi.org/10.1007/BF00649615

[29] M.R. Zaghloul and A.N. Ali, Algorithm 916: computing the Faddeyeva and Voigt functions. ACM Trans. Math. Software, 38 (2011) 15:1-15:22. http://dx.doi.org/10.1145/2049673.2049679

[30] W.H. Press, S.A. Teukolsky, W.T. Vetterling and B.P. Flannery, Numerical recipes in C. The art of scientific computing, Cambridge University Press, 2^{nd} ed., 1992.

[31] C. Chiarella and A. Reichel, On the evaluation of integrals related to the error function. Math. Comput., 22 (101) (1968) 137-143. http://www.jstor.org/stable/2004771

[32] S.M. Abrarov and B.M. Quine, Master-slave algorithm for highly accurate and rapid computation of the Voigt/complex error function, J. Math. Research, 6 (2) (2014) 104-119. http://dx.doi.org/10.5539/jmr.v6n2p104

[33] S.M. Abrarov and B.M. Quine, Sampling by incomplete cosine expansion of the sinc function: Application to the Voigt/complex error function, Appl. Math. Comput., 258 (2015) 425-435. http://dx.doi.org/10.1016/j.amc.2015.01.072

[34] S.M. Abrarov and B.M. Quine, Efficient algorithmic implementation of the Voigt/complex error function based on exponential series approximation, Appl. Math. Comput., 218 (5) (2011) 1894-1902. http://dx.doi.org/10.1016/j.amc.2011.06.072

[35] H. Amamou, B. Ferhat and A. Bois, Calculation of the Voigt Function in the region of very small values of the parameter a where the calculation is notoriously difficult, Amer. J. Anal. Chem., 4 (2013) 725-731. http://dx.doi.org/10.4236/ajac.2013.412087

[36] S.M. Abrarov and B.M. Quine, Accurate approximations for the complex error function with small imaginary argument, J. Math. Research 7 (1) (2015) 44-53. http://dx.doi.org/10.5539/jmr.v1n1p44

[37] S.M. Abrarov and B.M. Quine, A new application of the Fourier transform for rational approximation of the complex error function, arXiv:1511.00774. http://arxiv.org/pdf/1511.00774v1.pdf

[38] T.M. Karbach, G. Raven and M. Schiller, Decay time integrals in neutral meson mixing and their efficient evaluation, arXiv:1407.0748. http://arxiv.org/pdf/1407.0748v1.pdf

[39] W.B. Jones and W.J. Thron, Continued fractions in numerical analysis. Appl. Num. Math., 4(2-4) (1988) 143-230. http://dx.doi.org/10.1016/0168-9274(83)90002-8

[40] G.P.M. Poppe and C.M.J. Wijers, More efficient computation of the complex error function. ACM Transact. Math. Software, 16 (1990) 38-46. http://dx.doi.org/10.1145/77626.77629

[41] G.P.M. Poppe and C.M.J. Wijers, Algorithm 680: evaluation of the complex error function. ACM Transact. Math. Software, 16 (1990) 47. http://dx.doi.org/10.1145/77626.77630

[42] L.S. Rothman, I.E. Gordon, Y. Babikov, A. Barbe, D.C. Benner, P.F. Bernath, M. Birk, L. Bizzocchi, V. Boudon, L.R. Brown, A. Campargue, K. Chance, E.A. Cohen, L.H. Coudert, V.M. Devi, B.J. Drouin, A. Fayt, J.-M. Flaud, R.R. Gamache, J.J. Harrison, J.-M. Hartmann, C. Hill, J.T. Hodges, D. Jacquemart, A. Jolly, J. Lamouroux, R.J. Le Roy, G. Li, D.A. Long, O.M. Lyulin, C.J. Mackie, S.T. Massie, S. Mikhailenko, H.S.P. Müler, O.V. Naumenko, A.V. Nikitin, J. Orphal, V. Perevalov, A. Perrin, E.R. Polovtseva and C. Richard, The HITRAN2012 molecular spectroscopic database, J. Quant. Spectrosc. Radiat. Transfer, 130 (2013) 4-50. http://dx.doi.org/10.1016/j.jqsrt.2013.07.002

[43] S.M. Abrarov and B.M. Quine, A rational approximation for efficient computation of the Voigt function in quantitative spectroscopy, J. Math. Research, 7 (2) (2015), 163-174. http://dx.doi.org/10.5539/jmr.v7n2p163